EPJ Web of Conferences **380**, 01010 (2026) https://doi.org/10.1051/epjconf/202638001010
ICISCT'25

Compact and Flexible Two-Port MIMO Antenna for UWB Wearable Applications

Abderahman Tribak [1*], Asmaa Zugari[1] and Aziz Dkiouak [2]

[1]Intelligent Systems Design Laboratory, FS, Abdelmalek Essaadi University, 93002 Tetouan, Morocco.
[2] STIC Laboratory, FS,Chouaib Doukkali University, 24000, El Jadida, Morocco

Abstract. This paper is about a kind of antenna called a two-port MIMO antenna. It is designed for devices that people wear, like fitness trackers or smartwatches and it works well for communication over a wide range of frequencies from 3.5 to 11 GHz. The two-port MIMO antenna is small and flexible which makes it perfect for devices. It also works well electrically which means it can send and receive signals clearly. The two-port MIMO antenna has something called an envelope correlation coefficient or ECC which's very low, below 0.002. This means that the antenna is very good at sending and receiving signals and it does not get mixed up. The diversity gain of the two-port MIMO antenna is 10 dB, which is very good and means that it can send signals reliably even when there are a lot of obstacles around. The two-port MIMO antenna also has good isolation, which is better than −16 dB. This means that the signals sent by one part of the antenna do not interfere with the signals sent by the part. The total active reflection coefficient or TARC of the two-port MIMO antenna is below −10 dB and the reflection coefficient or S11 is also below −10 dB. This means that the antenna is very good at sending and receiving signals without losing any of the signal. The two-port MIMO antenna is very small 40 × 26 mm² but it works very well and is also flexible. This makes it perfect for devices that people wear. The channel capacity loss or CCL of the two-port MIMO antenna is below 0.4 bps/Hz, which means that it can send and receive signals quickly and reliably. This makes the two-port MIMO antenna perfect, for performance wearable devices.

1 Introduction

Smart clothing has gained significant traction recently due to its ability to incorporate wearable electronics such as smartwatches, electronic buttons, military berets, and sun-

* Abderahman Tribak: Abderahman.tribak@etu.uae.ac.ma

glasses. For such applications, it is essential that electronic components integrated into fabrics remain both flexible and adaptable to body movements. This evolution has led to the growth of smart garments, where wearable antennas are critical for wireless communication by enabling both data transmission and reception. These antennas are widely utilized in various sectors like healthcare, defense, medical monitoring, and even fashion design. For example, a security-oriented antenna was presented in [1],While the design was constrained by a narrow bandwidth, addressing this challenge has made the integration of compact antennas with broad operational frequency ranges cru-cial for wearable devices. Employing materials with low dielectric constants minimizes surface wave losses and improves the efficiency of signal transmission. For instance, a textile antenna presented in [2] demonstrates this approach effectively with a polyester base was studied to evaluate how the weaving process affects its functionality. Similarly, [3] proposed a flexible spiral antenna constructed with conductive threads that operated within the 1–3 GHz range. Another design featured a dual-port embroidered antenna tailored for military applications [4]. Other studies [5] explored the use of flexible, low-cost materials Examples of materials that are readily incorporated into everyday clothing include polydimethylsiloxane (PDMS), jeans, denim, cotton, felt and jute.To improve isolation and reduce coupling effects, several strategies have been developed. These include incorporating slits, slots, or specialized isolation structures [6], introducing parasitic elements between antenna elements [7], and using defected ground structures (DGS) [8]. Moreover, employing meandered ground lines has shown effectiveness in minimizing coupling [8]. A miniaturized wideband MIMO an-tenna designed for wearable use is introduced in this study. The isolation is achieved without introducing parasitic elements. The suggested antenna provides a DG of 10 dB, a ECC of less than 0.002, TARC below -10 dB and CCL remains below 0.4 bps/Hz. Therefore, the reflection coefficient of the electrical model and CST simulation results shows an acceptable agreement.

2 Antenna Element Design

Figure 1 presents the development stages of the wideband MIMO antenna. The antenna structure is realized on a jean's substrate, characterized by a relative permittivity ε_r of 1.6, a tan δ of 0.02, and a thickness of 1.5 mm. The complete antenna measures approximately 26 mm in width and 40 mm in length. The ground plane is fabricated from copper, with a thickness of 0.035 mm. To enhance the antenna's performance, a comprehensive parametric analysis was conducted using CST simulation software. Based on this study, the optimal dimensions of the wideband antenna were finalized: Ws=40mm, Ls=26mm, WF=3mm, Lf=10mm, r1=7mm, r2=2mm, a=4mm, b=2mm, c=6mm, ws1=38mm, d=16mm, g=10mm

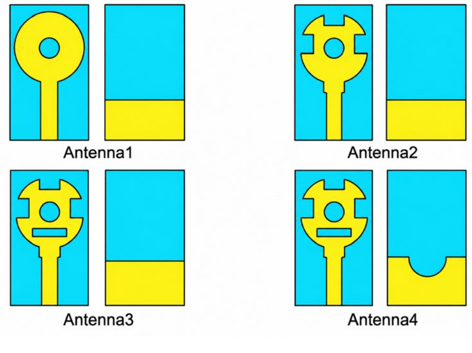

Fig. 1. Development stages of the antenna

The proposed antenna follows a four-stage design approach. In the first stage, a circular slot is introduced at the center of a standard microstrip patch to initiate performance tuning. In the second phase, three semi-rectangular cutouts are implemented in the radiating structure to further refine the response. During the third stage, a rectangular slot is placed underneath the initial circular one to improve isolation. Lastly, a semi-circular groove is engraved on the ground plane to optimize inter-element isolation and overall antenna efficiency. Figure 2 presents the S11 parameter variations across each stage of the design.

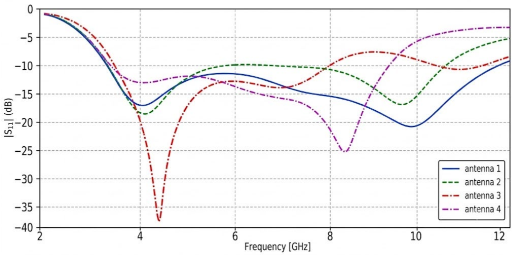

Fig. 2. Reflection coefficients at various stages of evolution.

3 Results And Interpretation

In the subsequent design stage, two identical antenna elements were positioned side by side to realize a MIMO configuration capable of operating over the 3.5–11 GHz frequency range. The proposed MIMO antenna layout is presented in Figure 3, while the corresponding S-parameter characteristics are depicted in Figure 4. The antenna demonstrates an isolation level better than −16 dB throughout the entire ultra-wideband (UWB) spectrum. As illustrated in Figures 5 and 6, the antenna shows strong performance in terms of both efficiency and gain. At 3 GHz, the simulated gain is approximately 1.1 dB, which increases to 3.54 dB at 7 GHz and reaches 4.6 dB at 10 GHz. The design further achieves a peak efficiency of 71.54%.

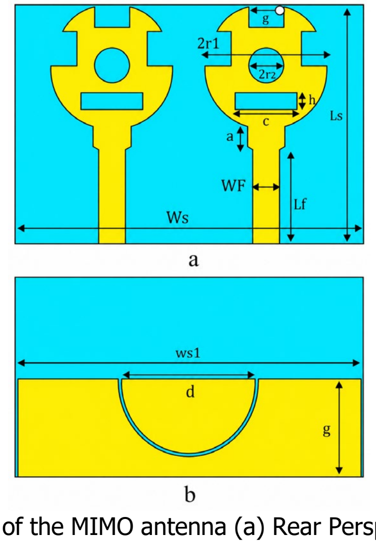

Fig. 3. Organization of the MIMO antenna (a) Rear Perspective, (b) Reverse View

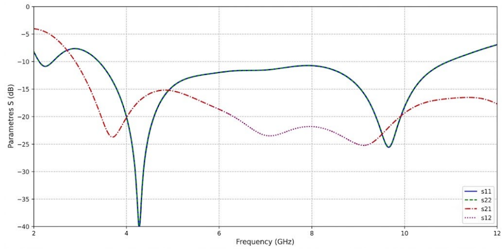

Fig. 4. Sij-plots of the This work's MIMO antenna

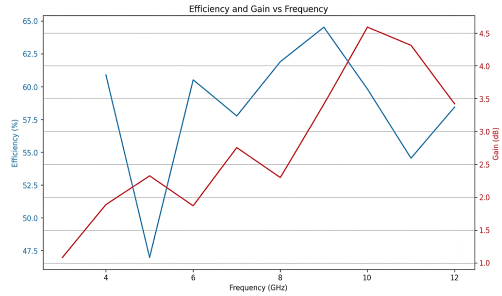

Fig. 5. efficiency and Realized gain of the proposed MIMO antenna

The electrical equivalent model is a valuable method for analyzing the behavior of antennas by representing them with lumped components such as resistors, inductors, and capacitors. This approach offers a more intuitive understanding of the antenna's function , According to previous studies resonators are often modeled as parallel RLC circuits. Based on this principle, an equivalent circuit was developed for a single antenna element. In this representation, the patch antenna is represented by an equivalent RLC circuit, where the resistance (R) signifies the radiation resistance, while the inductance (L) and capacitance (C) reflect the reactive components that in-fluence the resonant frequency. This circuit-based representation of the antenna system is depicted in Figure 6. Optimization of the model was carried out using Keysight ADS (Advanced Design System), with the corresponding component values detailed in the same figure. To ensure accuracy, the model's performance was validated against results from full-wave electromagnetic simulations. As illustrated in Figure 6, the in-put impedance values from both methods aligned closely, supporting the reliability of the circuit model.

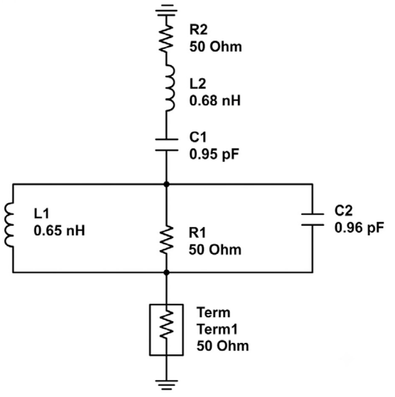

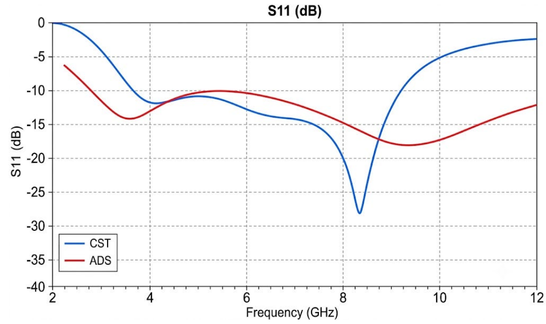

Fig. 6. Single-element antenna's equivalent

Substituting $L1 = 0.65$ nH, $L2 = 0.68$ nH, $C1 = 0.95$ pF, $C2 = 0.96$ pF, and $R1 = 50\ \Omega$ into equations (8)-(12) [9], the only real value for the angular frequency (ω) is 611152.33009 rad/s. Therefore, dividing the angular frequency by 2π gives the resonant frequency f = ω /2π = 3.84 GHz. The optimized values for the parameters R, L, and C are associated with the patch element shown in Figure 7 considering $R2 = 50\ \Omega$. The calculated reflection coefficient for the single patch using CST and the Keysight ADS simulator is If the figure shows a circuit design that the antenna exhibits broadband resonance characteristics in the CST simulation results, while a consistent resonance was observed in the measurements in the circuit analysis. The bandwidth match be-tween the CST and circuit results is found to be in good agreement .

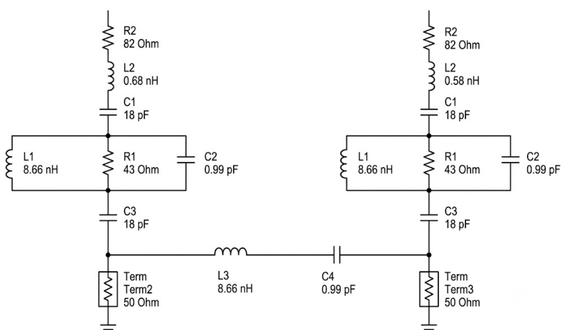

(a)

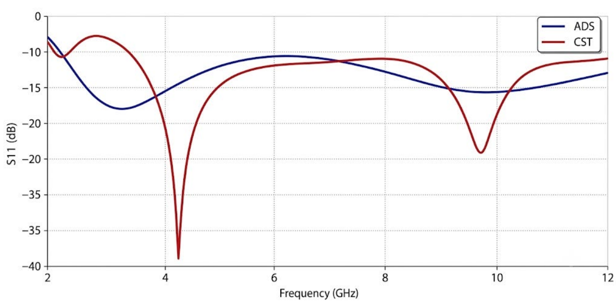

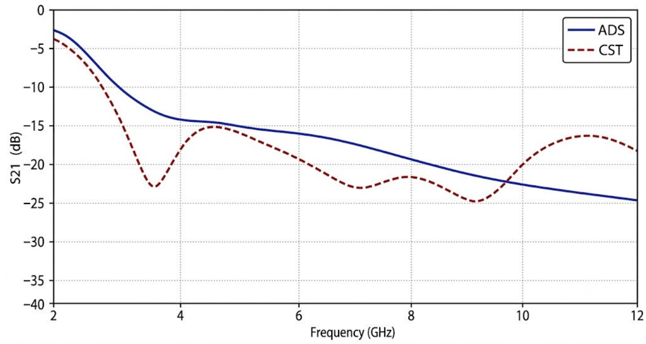

(b)

Fig. 7. Two-element MIMO antennas: (a) equivalent circuit model, (b) reflection coefficient comparison (CST and ADS results), and transmission coefficient comparison

Building upon the single patch element model, the equivalent circuit for the two element MIMO antenna was constructed and optimized through simulation in Keysight ADS. Two patches are described by the series arrangement of RLC parallel and RLC series model ($R1L1C1$and $R2L2C2$for patch 1 and $R3L3C3$and $R4L4C4$for patch 2). The optimized R, L and C values for each patch configuration are identical to those of the single patch element. The interconnection of the antenna elements is characterised by the following parameters $L5C5$ series The antenna's calculated reflection and transmission coefficients using CST and the Keysight ADS simulator (for L_5= 7.55 nH and C_5= 0.85 pF). The figure 8 show that the ADS results almost follow the CST results

4 MIMO Performance Parameters

Throughout this part of the study the proposed MIMO antenna is investigated by evaluating key parameters that are essential for characterizing the performance of the MIMO system. These parameters include DG and ECC, which indicate signal quality and spatial isolation. We have also evaluated the TARC, which determines the impedance matching efficiency under simultaneous port excitation, and the CCL, which in turn quantifies the reduction in system throughput due to inter-element coupling and correlation. Together, these metrics provide a holistic view of antenna behavior in real-world multi-antenna uses.

4.1 Envelope Correlation Coefficient (ECC)

The attainment of optimal MIMO performance is contingent upon the analysis. ECC serves as an essential indicator for evaluating the diversity performance of antenna systems. It reflects how independent or correlated the signals are between different channels in a MIMO configuration. In multi-antenna systems, the ECC is computed by Analyzing how the radiation pattern of one antenna element impacts the others is crucial for understanding mutual coupling in antenna arrays. A lower ECC signifies better isolation between elements and improved diversity performance. for a two-port system, ECC can be derived using the far-field radiation patterns (as shown in Equation 1) or based on S-parameters (transmission/reflection coefficients) as shown in equation 2, In this context, $F1(\theta, \varphi)$ refers to the far-field response of the first antenna when only its port is activated, while Ω represents the solid angle over which the radiation pattern is integrated. In practice, it is imperative that the value of ECC is less than 0.5 [10]. In our antenna, the ECC value is observed to be in close proximity to zero, as shown in the graph. The ECC is good, as demonstrated in Figure 8.

$$ECC = \frac{\left|\int_{\Omega} F_1(\theta,\phi) F_2^*(\theta,\phi) d\Omega\right|^2}{\left(\int_{\Omega} |F_1(\theta,\phi)|^2 d\Omega\right)\left(\int_{\Omega} |F_2(\theta,\phi)|^2 d\Omega\right)} \quad (1)$$

$$ECC = \frac{|S_{12} + S_{21}|^2}{(1 - |S_{11}|^2)(1 - |S_{22}|^2)} \quad (2)$$

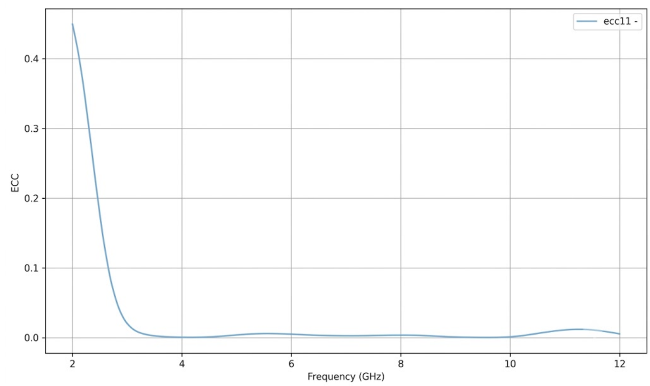

Fig. 8. ECC of the Presented MIMO antenna.

4.2 Diversity Gain (DG)

The phenomenon of d (DG) is typically realized when multiple versions of the transmitted signal are received through various propagation paths. It is generally accepted that a diversity gain value approaching 10 dB is indicative of excellent diversity performance. The aforementioned gain can be derived from the envelope correlation coefficient, as demonstrated in Equation (3).

$$\mathrm{DG} = 10\sqrt{1 - (\mathrm{ECC})^2} \quad (3)$$

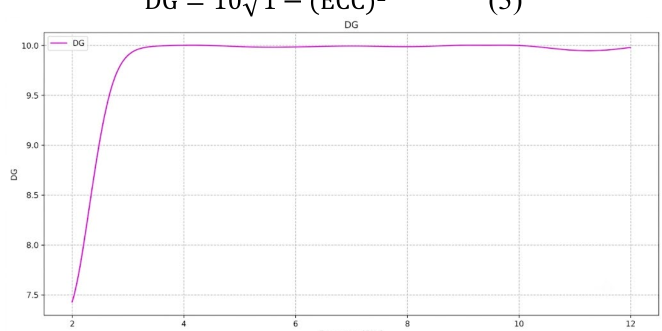

Fig. 9. Diversity Gain Analysis of the Proposed Antenna

4.3 Total Active Reflection Coefficient (TARC)

TARC is a key parameter used to evaluate the performance of multi-port antennas, particularly in MIMO systems. It provides an indication of the degree of mutual coupling and independence between antenna ports. A lower TARC value indicates better isola-tion and reduced coupling, which is desirable in MIMO configurations to maintain channel independence. TARC is mathematically defined as the square root of the sum of the squares of the active reflection coefficients [10], as shown in equation (4), where the excitation phase θ varies from 0 to 2π, the graph in figure 10 illustrates the TARC response over a frequency range from 3.5 GHz to 11 GHz. It can be seen that the TARC drops below -10 dB at several frequency points, indicating good isolation and minimal reflection, confirming the effectiveness of the antenna design in maintaining port de-coupling over the operating band [11].

$$\text{TARC} = \sqrt{\left|S_{11} + Se_{12}^{i\theta^2}\right| + \left|S_{21} + Se_{22}^{j\theta^2}\right|}/\sqrt{2} \qquad (4)$$

Where θ is varied from 0 to 2π

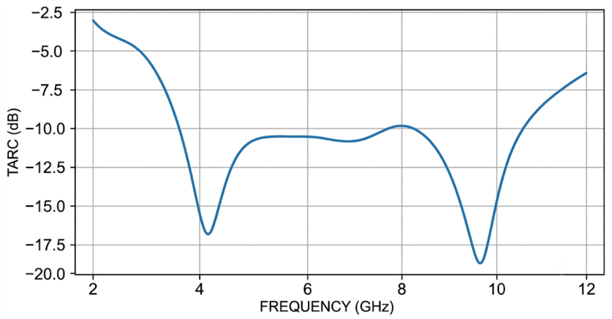

Fig. 10. TARC of This work's MIMO antenna.

4.4 Channel Capacity Loss (CCL)

CCL is an important parameter in evaluating MIMO antennas as per the standard threshold, CCL should remain below 0.4 bps/Hz. For our MIMO antenna, the CCL is observed to be nearly zero at 9.8 GHz. Across the frequency range extending to 12 GHz, the CCL consistently stays within the acceptable limits. The calculations for CCL are performed using Equations (5) and (6), with the results illustrated in Figure 11.

$$C_{\text{Loss}} = -\log_2 \det[\alpha^R]$$

$$[\alpha^R] = \begin{bmatrix} \alpha_{11} & \alpha_{12} \\ \alpha_{21} & \alpha_{22} \end{bmatrix} \qquad (5)$$

$$\alpha_{11} = 1 - (|S_{11}|^2 + |S_{12}|^2) \qquad (6)$$

$$\alpha_{12} = S_{11}S_{12} + S_{21}S_{12}$$

$$\alpha_{21} = S_{22}S_{21} + S_{12}S_{21}$$

$$\alpha_{22} = 1 - (|S_{22}|^2 + |S_{21}|^2)$$

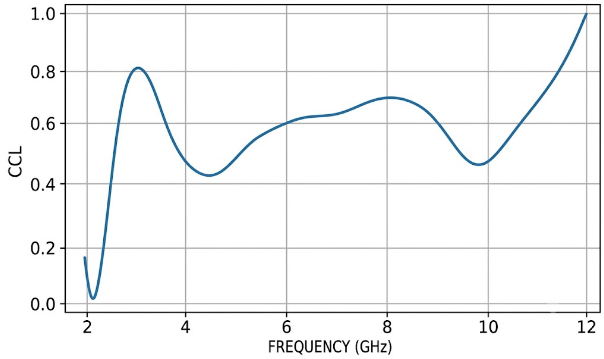

Fig. 11. CCL response of the presented MIMO antenna

5 Comparison of Another Researcher's Work

A comparative analysis was conducted to evaluate the performance of the proposed MIMO antenna, focusing on port isolation, bandwidth coverage, and radiation gain. As demonstrated in Table 1, The designed antennas offer adequate isolation but often have larger physical dimensions or limited bandwidth. It has been demonstrated that wideband designs are prone to poor isolation, which can negatively impact the performance of MIMO systems. In contrast, the proposed antenna exhibits strong port isolation, extensive frequency coverage, and efficient radiation gain. The compact design of the device makes it ideal for space-constrained applications, offering optimized performance for reliable MIMO systems.

Table 1. Performance evaluation of the proposed design against those of the previous literature

Ref.	Ports	Substrate	Isolation (dB)	Bandwidth	Size (mm)	DG (dB)	ECC	Gain (dB)
[12]	2	Jeans (1.6)	>12	3.6–7 GHz	40 × 50	na	0.025	6.5
[13]	4	Jeans (1.6)	>20	3.4–11.8 GHz	56 × 41	>9.99	<0.002	4.3
[14]	2	Textile (1.2)	>12	2.3–2.8 GHz	38.1 × 38.1	na	na	2.79
Proposé	2	Jeans (1.6)	>16	3.5–11 GHz	40 × 26	10	<0.002	4.6

6 Conclusion

This article presents a two-port flexible MIMO antenna designed for integration into wearable technology systems. The antenna demonstrates excellent inter-element isolation, maintaining S-parameters below −16 dB across the operating band and ensuring effective impedance matching, with S(ii) remaining under −10 dB throughout the 3.5–11 GHz frequency range. To evaluate performance, key MIMO metrics such as ECC, DG, TARC, and CCL were analyzed. The results confirm that the antenna delivers strong MIMO characteristics across the entire band, underscoring its potential for future wearable communication system applications. The key innovation of this study lies in the development of a compact and flexible two-port MIMO antenna optimized for ultrawideband wearable uses. Compared with conventional models, this design ensures higher isolation and reduced mutual coupling without relying on additional decoupling structures or parasitic elements. Moreover, it maintains high diversity and minimal correlation across the operating band, making it highly suitable for efficient, space-limited smart textile platforms.

References

1. S. Costanzo and G. Ammendola, "Compact textile wearable antenna for security applications," presented at IEEE Conference, Dubrovnik, Croatia, Sept. 2019, pp. 1–3. (Conference paper).
2. R. Aprilliyani, P. A. Dzagbletey, J. H. Lee, M. J. Jang, J.-H. So, and J.-Y. Chung, "Effects of Textile Weaving and Finishing Processes on Textile-Based Wearable Patch Antennas," IEEE Access, vol. 8, pp. 63295–63305, 2020. https://doi.org/10.1109/ACCESS.2020.2983912
3. J. Zhong, A. Kiourti, T. Sebastian, Y. Bayram, and J. L. Volakis, "Conformal Load-Bearing Spiral Antenna on Conductive Textile Threads," IEEE Antennas and Wireless Propagation Letters, vol. 18, no. 11, 2019. https://doi.org/10.1109/LAWP.2019.2944700
4. A. K. Biswas, K. Roy, and U. Chakraborty, "Investigation of a Four-Element Textile MIMO Antenna for Ku-Band Applications," Proc. IEEE Region 10 Symposium (TENSYMP), Dhaka, Bangladesh, 2020. https://doi.org/10.1109/TENSYMP50017.2020.9230630
5. H. Ben Hamadi, S. Ghnimi, L. Latrach, and A. Gharsallah, "Design of Millimeter-Wave Textile Antenna Loaded with AMC Structures for 5G Applications," Proc. 32nd International Conference on Microelectronics (ICM), 2020. https://doi.org/10.1109/ICM50269.2020.9331808
6. H. Arun, A. K. Sarma, M. Kanagasabai, S. Velan, C. Raviteja, and M. G. N., "Deployment of Modified Serpentine Structure for Mutual Coupling Reduction in MIMO Antennas," IEEE Antennas and Wireless Propagation Letters, vol. 19, no. 11, 2020. https://doi.org/10.1109/LAWP.2020.3026906
7. A. Iqbal, A. Smida, A. J. Alazemi, M. I. Waly, N. Khaddaj Mallat, and S. Kim, "Wideband Circularly Polarized MIMO Antenna for High Data Wearable Biotelemetric Devices," IEEE Access, vol. 8, 2020. https://doi.org/10.1109/ACCESS.2020.2968153
8. C. G. Revati and R. R. Patil, "Slot-Based Mutual Coupling Reduction Technique for MIMO Antenna," SN Computer Science, vol. 2, 2021. https://doi.org/10.1007/s42979-021-00483-6
9. I. Elfergani, A. Iqbal, C. Zebiri, et al., "Low-Profile and Closely Spaced Four-Element MIMO Antenna for Wireless Body Area Networks," Electronics, vol. 9, no. 2, 258, 2020. https://doi.org/10.3390/electronics9020258
10. R. Pandey, A. K. Biswas, and U. Chakraborty, "Compact Body-Worn MIMO Antenna with High Port Isolation for UWB Applications," International Journal of Communication Systems, vol. 37, no. 9, 2024. https://doi.org/10.1002/dac.5820
11. A. Dkiouak, M. El Ouahabi, A. Zakriti, et al., "Design of Four-Element MIMO Antenna System for Intelligent Internet of Everything (IIoE)," Telecommunication Systems, vol. 86, pp. 559–570, 2024. https://doi.org/10.1007/s11235-024-01204-8

12. P. Pradeep, M. M. Basha, S. Gundala, et al., "Development of Wearable Textile MIMO Antenna for Sub-6 GHz Band New Radio 5G Applications," Micromachines, vol. 15, no. 5, 651, 2024. https://doi.org/10.3390/mi15050651
13. V. K. Jhunjhunwala et al., "A Four-Port Flexible UWB MIMO Antenna with Enhanced Isolation for Wearable Applications," Results in Engineering, 2024. https://doi.org/10.1016/j.rineng.2024.103197
14. H. Li, S. Sun, B. Wang, and F. Wu, "Design of Compact Single-Layer Textile MIMO Antenna for Wearable Applications," IEEE Transactions on Antennas and Propagation, vol. 66, no. 6, 2018. https://doi.org/10.1109/TAP.2018.2819706
15. S. Kumar, K. Srivastava, S. Kumar, D. Sharma, R. N. Tiwari, A. Kandwal, M. K. Singh, and B. Goyal, "Design and Implementation of High Isolation Textile MIMO Antenna for Wearable Applications," International Journal of Communication Systems, vol. 38, no. 4, 2025. https://doi.org/10.1002/dac.70052